Journal of Visualization, Vol. 8, No. 1 (2005)49-56

Flow Patterns of Cross-Flow around a Varicose Cylinder

Wang, F. H.*[1], Jiang, G. D.*[2] and Lam, K.*[3]

*1 School of Energy and Power Engineering, Xi'an Jiaotong University, Xi'an, Shaanxi, 710049, P. R. China. E-mail: fhwang@mail.xjtu.edu.cn
*2 School of Mechanical Engineering, Xi'an Jiaotong University, Xi'an, Shaanxi, 710049, P. R. China.
*3 Department of Mechanical Engineering, The Hong Kong Polytechnic University, Hung Hom, Kowloon, Hong Kong.

Received 8 May 2004
Revised 1 July 2004

***Abstract*:** The near wake of a varicose cylinder has been experimentally investigated using Laser Induced Fluorescence (LIF) and Digital Particle Imaging Velocimetry (DPIV). The work aims to provide understanding to the mechanism of the cross flow around varicose cylinder as well as to comprehend why the introduction of relatively small degrees of spanwise waviness can have a significant effect on drag reduction and suppression of the cylinder vibration. The evolution of the flow patterns and the corresponding vortex interactions are obtained. The experimental results indicated that the wake width and the formation length vary along the span of the varicose cylinder. A wider wake and a longer formation length were observed in the saddle plane. In addition, an interpretation of the three-dimensional wake structures is postulated and conceptually shown. The numerical simulation by 3-D finite volume method is successful in predicting the flow features found by the experiments.

***Keywords*:** Varicose Cylinder, PIV, LIF, CFD, Flow Pattern.

1. Introduction

Above some critical Reynolds number, vortex shedding from nominally two-dimensional bluff bodies exhibits certain three-dimensional characteristics, irrespective of how carefully the experiment is carried out. In the past decade, many measurements have been carried out to study the three-dimensionality of the cylinder wake over a wide range of Reynolds number by Gerrard (1978), Wei and Smith (1986), Wu et al. (1996), Williamson (1996), Tombazis & Bearman (1997) and Owen & Bearman (2001), etc. All of these investigations have provided valuable insight on the three-dimensional aspects of vortex shedding from a bluff body.

Over past several decades, a number of passive methods were also proposed to reduce the drag force and the magnitude of the periodic fluctuating force resulting from regular vortex shedding with the aim of lessening or even suppressing VIV (Vortex-Induced-Vibration). These techniques entail modification of the body geometry and most often involve the introduction of some forms of three-dimensional geometric disturbance to the base form of a nominally two-dimensional bluff body, for examples, helical strakes, ribbons, bumps, etc.

Recently, Lam et al. (2004) proposed a new type cylinder, varicose cylinder, and found that it is an omni-directional method to reduce the mean drag force and the associated vibration amplitude. Wang et al. (2004) investigated the mean and fluctuating velocity components in the near wake of a varicose cylinder using Laser Doppler Anemometer. They found that the wake in the saddle plane

has a longer vortex formation region and a rapider reverse flow as well as the spanwise flow is from the saddle plane towards the nodal plane on both sides of the varicose cylinder. Their results also show that the wake of the varicose cylinder is more incoherent turbulence due to enhancement of turbulent mixing by the three-dimensional effects. Despite of the fact that some prominent features were obtained, an understanding of the flow behind varicose cylinder still poses a great challenge.

In this paper, we present experimental results in the form of flow visualization, aimed at understanding the physical structure of the vortex shedding from a varicose cylinder. It is hoped that this investigation will be helpful to comprehend why the introduction of relatively small degrees of spanwise waviness should have such a large effect on drag reduction and suppression of the cylinder vibration. The experiments were performed in a water tunnel. The facility is described in section 2. The results of LIF experiment as well as discussions are presented in section 3. The numerical simulations and comparison with experiments are given in section 4. Some conclusions were drawn in section 5.

2. Experimental Apparatus and Instrumentation

The experiments were conducted in a return-circuit water tunnel at Hong Kong Polytechnic University. Water is pumped through a straight measurement section containing a calibrated orifice flow meter, though a diffuser, into a settling chamber containing filter material and a honeycomb. The water then passes through a contraction and a straight square section before entering the working section. The working section is 480 mm long and 150 × 150 mm wide and has transparent walls made of acrylic. An inverter was used to control the speed of the centrifugal pump. The velocity in the working section could be continuously varied from 0 to 0.35 m/s. The Reynolds numbers in the experiments are 200 and 400 based on the free-stream velocity and the mean diameter of cylinder.

The cylinder model, shown in Fig. 1, was made of acrylic. The cylinder is 148 mm long with the mean diameter (D) of 17.6 mm. The saddle diameter is 14.4 mm and the nodal is 20.8 mm. The amplitude of the sinusoidal curve surface, a, is 1.6 mm. The wavelength, λ, is 40 mm. The cylinder was vertically installed in the water tunnel in a cantilever manner.

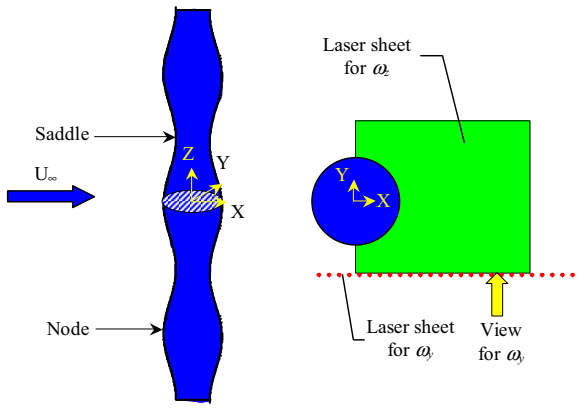

Fig. 1. The geometry of the varicose cylinder and orientations of the laser sheets.

In order to measure the instantaneous velocity field as well as to calculate the vorticity field from the velocity estimates, a digital PIV method was employed. Flow was seeded with particles, made of polyamide, which are white hollow microspheres with a mean diameter < 50 μm. A 4W Spectra-Physics Stabilite 2017 Argon-Ion laser was used to illuminate the near wake region behind the cylinder. The laser beam was pulsed using a scanning beam box, including a circular mirror, a rotating polygon mirror and a parabolic reflecting mirror. The scanning frequency of the laser sheet is continuously variable in the range of 78 to 1000 cycles per second. The digital images were recorded using an Adimec MX12P CCD camera with 1024 ×1024 pixels resolution and a Matrox

Pulsar frame grabber. The interrogation time is variable from 2.0 to 38.6 ms. The maximum frame rate is 25 images per second. The cross-correlation technique of the multi-frame single exposure method was adopted. The velocity field was extracted from the particle image using a VIDPIV software system based on the Young's fringe method.

The flow visualization technique is Laser induced fluorescence (LIF), in which a laser sheet is used to illuminate a fluorescent dye that is washed from the front face of the cylinder as the experiment is carried out to get the evolution of the flow patterns and their vortices interactions. The florescent dye is Rhodamine 6G (99%) with the maximum absorption wavelength of 530nm and the maximum emission wavelength of 560nm. The dye streak lines were illuminated using the same laser sheet and recorded with a JVC CCD video camera. The frame rate of this video camera is 25 f/s. The interrogation time is 8 ms.

3. Experimental Results and Discussion

Instantaneous in-plane flow field results of a nodal plane in the wake of the varicose cylinder are shown in Fig. 2, which were obtained from processing the DPIV particle images. The vorticity fields corresponding to the velocity fields are shown in the middle, while the streamlines obtained by integrating the velocity field, are shown in the right. Bilinear interpolation of the measured

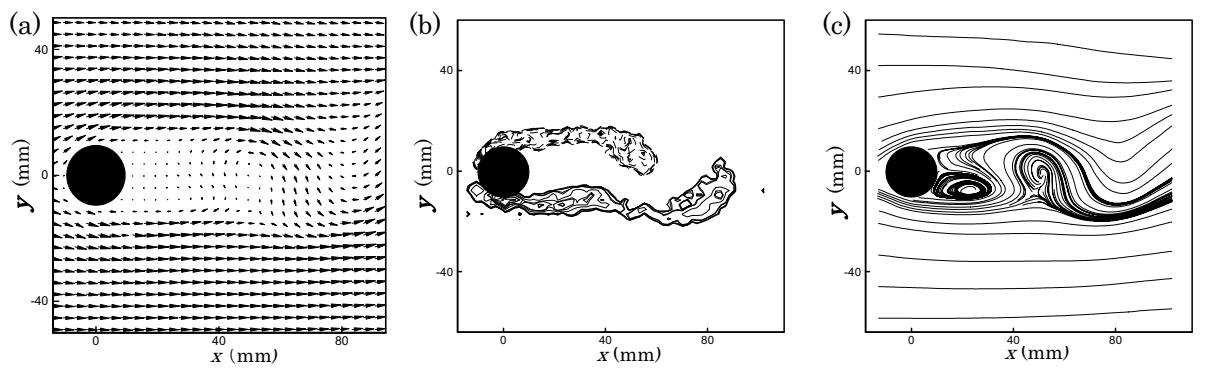

Fig. 2. Instantaneous in-plane flow field result in the wake of the varicose cylinder at a node plane, *Re*=200, derived from DPIV. (a) velocity fields; (b)vorticity contours; (c) streamlines.

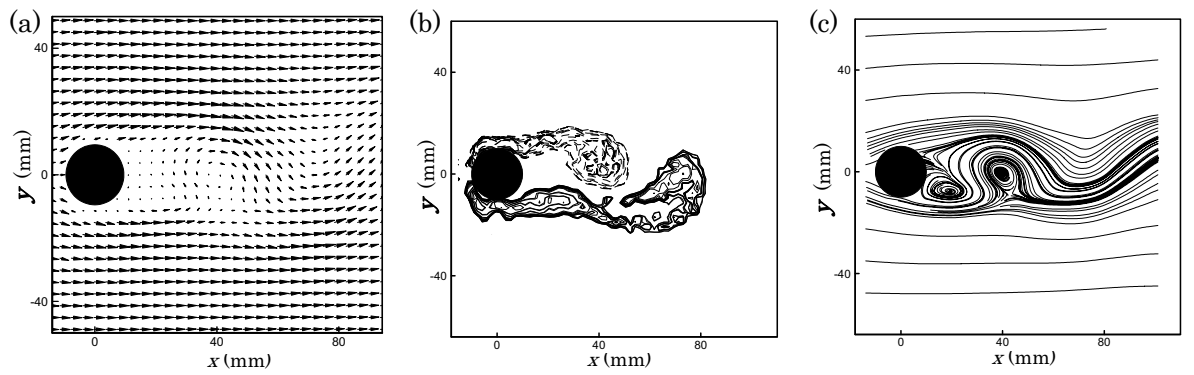

Fig. 3. Instantaneous in-plane flow field result in the wake of the varicose cylinder at a saddle plane, *Re*=200, derived from DPIV. (a) velocity fields; (b)vorticity contours; (c) streamlines.

velocity data was used in the integration. The Reynolds number is 200. From the vorticity contours map, the formation and evolution of the two rows of opposite-signed vortices forming the familiar Karman Street can be easily tracked. The generated distribution of vorticity has an elliptic structure. Features of the streamline pattern are that the separating free shear layers shed from the two sides are nearly in parallel. Figure 3 shows an instantaneous in-plane velocity field and the

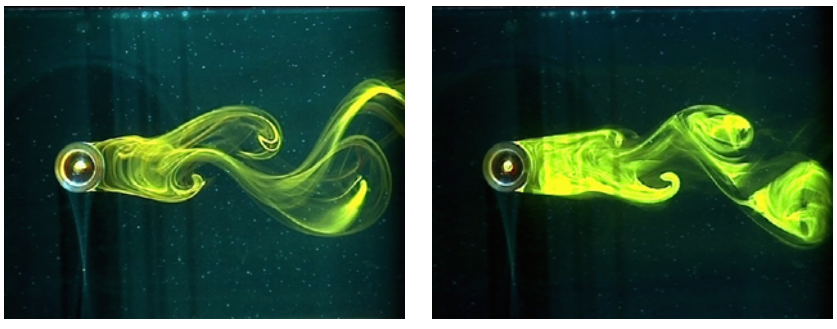

Re =200 *Re* =400

Fig. 4. Flow pattern in the near wake of a nodal plane.

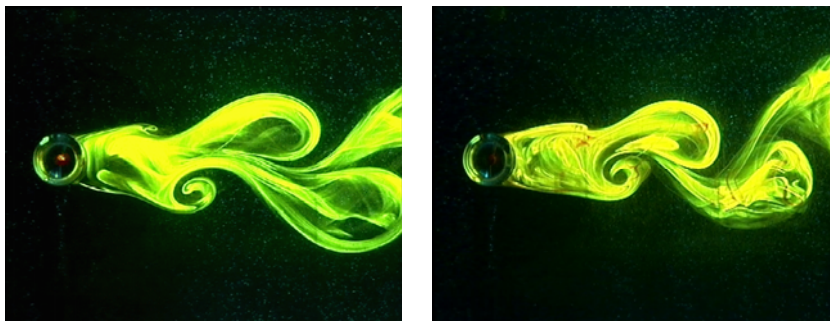

Re =200 *Re* =400

Fig. 5. Flow pattern in the near wake of a saddle plane.

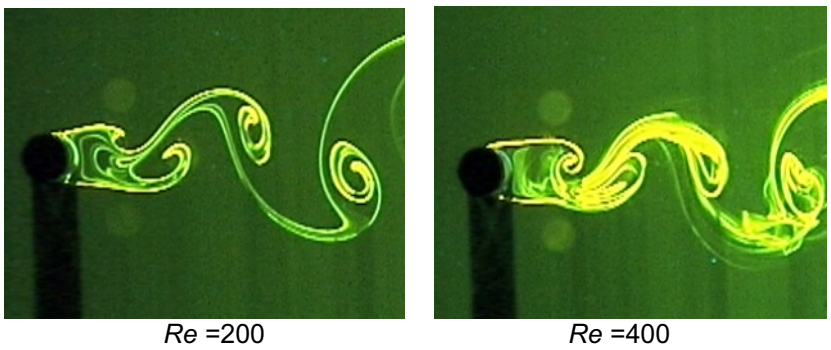

Re =200 *Re* =400

Fig. 6. Flow pattern in the near wake of a circular cylinder.

vorticity contours as well as streamlines in a saddle plane. The Reynolds number is same as in Fig. 2. From the vorticity contours map, it is found that the vorticity has a hook-like structure. This structure shows that the three-dimensional effects are stronger in the saddle plane than nodal plane. From streamlines pattern, it is evident that the wake in the saddle plane is wider than in the nodal plane, which validate the LDV results by Wang et al. (2004).

Typical flow patterns in the near wake of a nodal plane are shown in Fig. 4 obtained by LIF. The Reynolds number is 200 and 400, respectively. Unlike the flow pattern of a circular cylinder, the vortex shape behind the varicose cylinder curved up like a balloon. This feature is also found in the near wake of a saddle plane, shown in Fig. 5. From Figs. 4 and 5, it is evident that the near wake in the saddle plane is wider than that in the nodal plane. Although the LIF experiments were carried out at relatively low *Re*, the results were consistent with those deduced from velocity distribution measurements at higher *Re* by Wang et al. (2004); namely, the near wake width is wider in the saddle plane than in the nodal plane. Normally, a wider wake accompanies an earlier vortex separation. Therefore, separation in the saddle plane is earlier than in the nodal plane and this could also be identified from flow visualization pictures. To compare with flow pattern in the

near wake of a circular cylinder (Fig. 6), it can be found that the far wake of the varicose cylinder consists of elongated and attached vortices with much less pronounced waviness between two sides of opposing vorticity. The near-wake behind the varicose cylinder is very steady compared to the case of circular cylinder. The unsteady wake of the varicose cylinder seems to have been pushed away farther downstream. The steady near-wake is consistent with the force measurement results of small, but steady, lift coefficient (Lam et al., 2004).

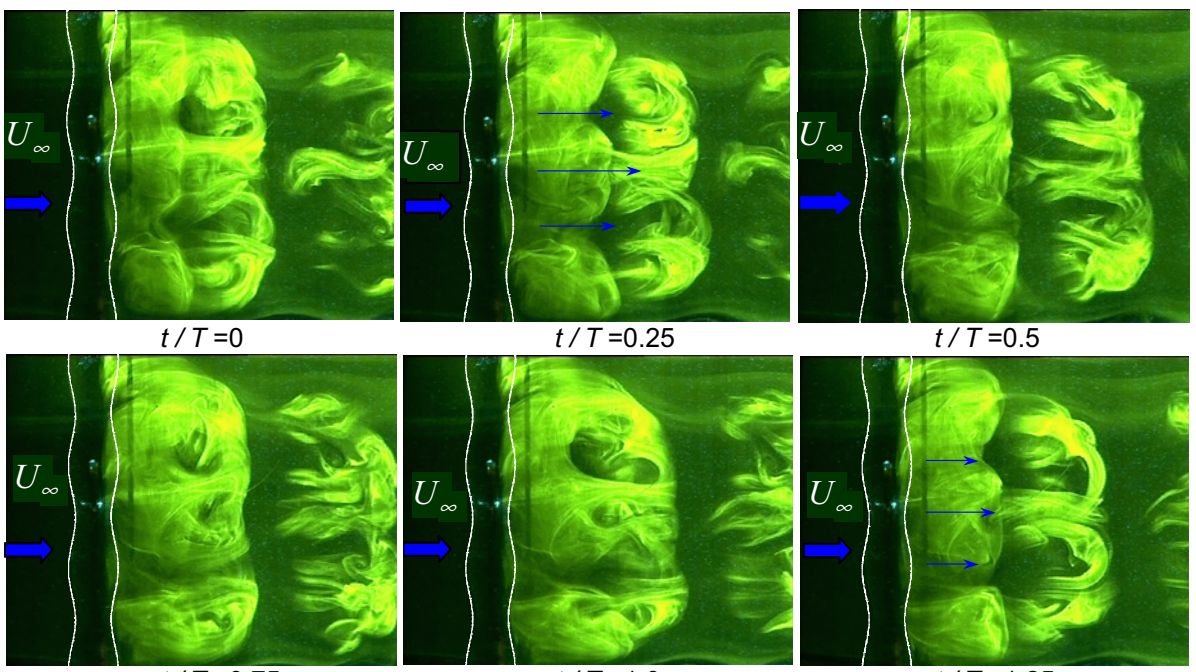

Fig. 7. A time sequences of LIF results on spanwise vortical structure of the varicose cylinder, *Re* =600.

Figure 7 shows the spanwise vortical structures obtained using LIF at *Re*=600 with the laser sheet orientation designated as ω_y in Fig. 1. Flow is from left to right. Because the cylinder is made of acrylic, it is difficult to found the cylinder from LIF photos; only the front of the cylinder is visible. From the figure, it can be observed that the formation length in the wake of the saddle plane is longer than that in the nodal plane, as indicated by the arrows. This 3-D phenomenon can be seen clearly after the Strouhal vortex has just been shed, for example, at t/T = 0.25 or 1.25, where t is the recording time and T is the period of the vortex shedding. In addition, a rib-like structure was found in the cylinder wake joining neighboring vortices. This is most obvious at t/T = 1.25. This three dimensional vortex caused the distortion of Strouhal vortex filament. The continuous distortion of vortex filaments led ultimately to their breakdown in the near wake. Gerrard (1978) observed the same distortions of vortex filaments in the wake of a circular cylinder and called them 'fingers' because they were pointed towards the cylinder. In his research, the fingers appeared at randomly disposed spanwise positions and followed each other in succession at the same spanwise position. As *Re* increased, these fingers appeared in clumps with a larger number of filaments and more frequently at each position. According to the description of 'fingers', it could be postulated that the rib-like structure in the present experiments might have the same structure as 'fingers'. However, the rib-like structure in the wake of a varicose cylinder seems to appear near the saddle planes. Furthermore, the number of structures is constant and is equal to the number of saddles of the cylinder. From the above observation, it could be deduced that the varicose shape caused the present structure of the wake to be different from that behind a circular cylinder. It is quite possible that, unlike a 2-D vortex sheet, the 3-D vortex sheet behind a varicose cylinder is more difficult to roll up into a mature vortex. Therefore, it rolls up at a position further downstream (thus a longer

formation length) with reduced strength. Such vortices then interact and break down through a rib-like structure. Traditionally, the drag force has been linked to the curvature of the separated shear layer. A shorter formation length usually implies a shear layer curving more rapidly towards the near wake centerline and this increased streamline curvature would have to be balanced by a larger pressure drop across the shear layer. In view of this consideration, this long vortex formation length found in the wake of saddle plane would bring about a beneficial result on drag reduction and suppression of vibration.

According to the above observation, two characteristics are noticeable in the flow structure: (1) free shear layer separation in the saddle plane is earlier than that in the nodal plane ($\alpha_s < \alpha_n$, where α_s denotes the separation angle in the saddle plane and α_n in the nodal plane); and (2) the near wake in the saddle plane is wider than that in the nodal plane and the vortex formation region in the saddle plane is longer than that in the nodal plane. A sketch of this 3-D flow structure is postulated in Fig. 8.

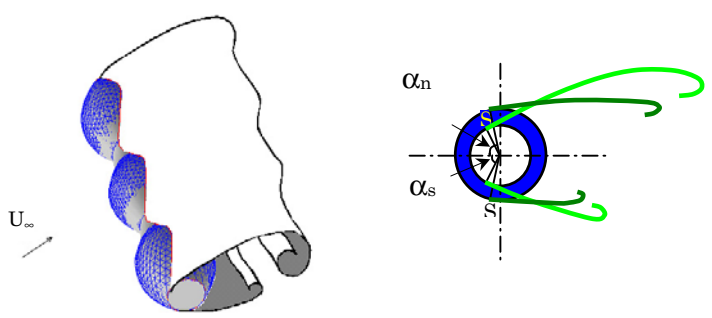

Fig. 8. A conceptual illustration showing the three-dimensional wake structures. α_s denotes the separation angle in saddle plane; α_n denotes the separation angle in nodal plane; S denotes the separation points.

4. Numerical Simulations and Comparison with Experiments

With the rapid development of powerful computers, numerical simulation visualization is becoming more and more popular. Compared with experiments, computational fluid dynamics (CFD) can get more detailed information about different kinds of flow fields, such as velocity fields, force histories and pressure distributions et al., which is very time consuming, expensive and sometimes even impossible to get accurate results. Based on this idea, the importance of three-dimensional effects arouses interest also in numerical studies. Several researchers (e.g., Dallmann et al., 1995; Darekar and Sherwin, 2001) have developed finite difference, finite element, spectral element and discrete vortex codes to simulate 3-D bluff body flows.

In the present study, the 3-D unsteady N-S equation is calculated using Finite volume solver of FLUENT 5.0 on an unstructured mesh with second-order implicit formulation and PISO (pressure-velocity coupling algorithm). The boundary conditions are set as uniform flow at inlet, no-slip for both varicose cylinder and sidewall of box, and out flow at exit. The initial flow field is assumed to be uniform and equal to inlet flow velocity. The Reynolds number, which equals to 176, is defined in terms of equivalent diameter of the cylinder and the uniform mainstream velocity. The equivalent diameter of the varicose cylinder is 17.6 mm and the wavelength, λ, is 40 mm. The cylinder is located along x axial. Uniform mainstream velocity U_∞ = 10 mm/s is parallel to z direction. The time-step of the simulation is 0.05 s. The computation domain is in a rectangular box of x = 0~160 mm, y = -110~110 mm, and z = -150~515 mm. An unstructured mesh with 1,006,432 tetrahedral cells and 180,908 nodes has been used. Three sub-domains are produced. One is between varicose cylinder and a concentric column surface of 30mm diameter. It is adopted to detail

the mesh near the varicose cylinder with 20,484 triangular faces on the varicose cylinder surface. Other sub-domains are created for the wake and for the far-field region. Solving the 3-D N-S equation until it became quasi-steady produced the computational results. From this point onwards, about 6 additional cycles were calculated.

Side and perspective views of the simulated wake patterns are demonstrated in Fig. 9, which is a group of path lines. The vorticity magnitude is indicated by the color gradation. As shown in the figure, a wide wake is present in the saddle plane and a narrow wake is observed behind a node. This phenomenon is in agreement with the experimental results. From the perspective view, it is found that there is a spanwise flow around the varicose cylinder. The free shear layers shed from the points near the saddles extend along the spanwise direction, while the shear layer near the nodes contracts, and the flow of the separated shear layer is accelerated around it. It is reasonable to think this spanwise flow results in the distortion of the free shear layer and ultimately the three-dimensional vortex structure is formed.

The success of the 3-D numerical simulation by finite volume method provide an opportunity to do more investigations on this type of cylinder flows due to its important characteristics of drag reduction and suppression of the FIV (Flow-Induced-Vibration). These works should enable, for instance, to identify the significance of the dimensionless parameters such as degree of obliqueness $a^2/(\lambda D)$ of varicose cylinder, to find the optimal shape of the varicose cylinder which will give greatest effects in drag reduction and FIV suppression at different Re, and to study the vortex shedding patterns of the varicose cylinder so as to understand the physics of drag reduction and FIV suppression, etc.

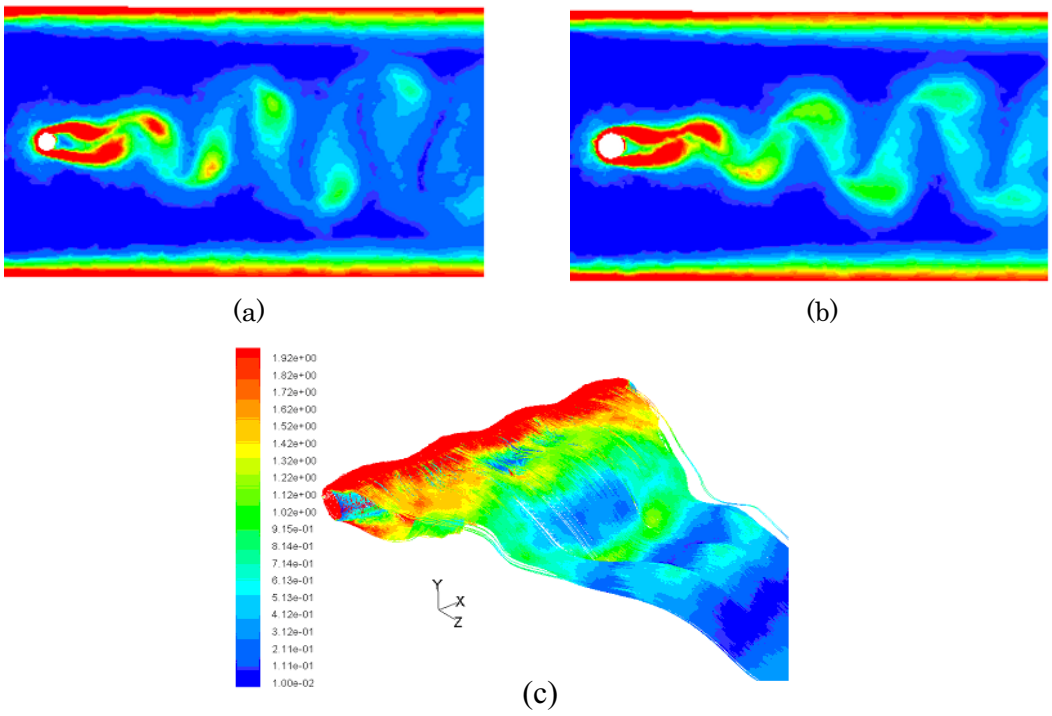

Fig. 9. Wake structures of the varicose cylinder in the cross flow by 3-D numerical simulation (a) In the wake of a saddle plane (b) In the wake of a Nodal plane (c) Panoramic view.

5. Conclusions

The main features of the three-dimensional near wake are the wake width and the formation length that varies along the span of the varicose cylinder. A wider wake and a longer formation length were observed in the saddle plane. Measurements from flow visualization and digital PIV

studies have also shown that the three-dimensional effect is stronger in the saddle plane, where there is a hook-like vorticity structure. In addition, a rib-like structure was observed in the spanwise wake. There are two distinct features comparing with the wake of the circular cylinder: one is the rib-like structure always appeared at the saddle positions; the other is the number of the structure is kept constant, which is equal to the saddle number of the cylinder. The numerical simulation by 3-D finite volume method is in agreement with the experimental results at low Reynolds number.

Acknowledgments

The work described in this paper was fully supported by a grant from the Research Grants Council of the Hong Kong Special Administrative Region, China (Project No. PolyU 5154/00E)

References

Dallmann, U., Herberg, T. H., Gebing, H., Su, W. H. and Zhang, H. Q., Flow field diagnostics: topological flow changes and spatio-temporal flow structure, AIAA Paper 95-0791, (1995).

Darekar, R. and Sherwin, S. J., Flow past a square section cylinder with a wavy stagnation face, Journal of Fluid Mechanics, 426 (2001), 263-294.

Gerrard, J. H., The wakes of cylinderical bluff bodies at low Reynolds number, Philosophical Transactions of the Royal Society of London, 288 (1978), 351-382.

Lam, K., Wang, F. H., Li, J. Y. and So, R. M. C., Experimental investigation of the mean and fluctuating forces of wavy (varicose) cylinders in a cross-flow, Journal of Fluids and Structures, 19 (2004), 321-334.

Owen, J. C. and Bearman, P. W., Passive control of VIV with drag reduction, Journal of Fluids and Structures, 15 (2001), 597-605.

Tombazis, N. and Bearman, P. W., A study of three-dimensional aspects of vortex shedding from a bluff body with a mild geometric disturbance, Journal of Fluid Mechanics, 330 (1997), 85-112.

Wang, F. H., Jiang, G. D. and Lam, K., A study of velocity fields in the near wake of a wavy (varicose) cylinder by LDA, Flow Measurement and Instrumentation, 15 (2004), 105-110.

Wei, T. and Smith, C. R., Secondary vortices in the wake of circular cylinders, Journal of Fluid Mechanics, 169 (1986), 513-533.

Williamson, C. H. K., Vortex dynamics in the cylinder wake, Annual Review of Fluid Mechanics, 28 (1996), 477-539.

Wu, J., Sheridan, J., Hourigan, K. and Soria, J., Shear layer vortices and longitudinal vortices in the near wake of a circular cylinder, Experimental Thermal and Fluid Science, 12 (1996), 169-174.

Author Profile

Fenghao Wang: He received his Ph.D. in Power Engineering and Engineering thermophysics in 1999 from Xi'an Jiaotong University. Then he worked in Department of Mechanical Engineering, Hong Kong Polytechnic University as a research assistant from 2001 to 2003. He works in School of Energy and Power Engineering, Xi'an jiaotong University as an associate professor since 2003. Now his research interests are flow around cylinders, flow visualization studies, fluid machines.

Gedong Jiang: She received her Ph.D. in Mechanical Engineering in 1998 from Xi'an Jiaotong university. She became an assistant professor at Xi'an Jiaotong university, and currently is an associate professor. She worked in Department of Mechanical Engineering, Hong Kong Polytechnic University as a research assistant from 2002 to 2003. Her current research interests are computational fluid dynamics.

Kit Lam: He Graduated from the Department of Mechanical Engineering of the University of Hong Kong in 1974 and obtained MPhil degree in fluid mechanics in 1977. He then worked in the bus company KMB as assistant engineer and lecturer of the Hong Kong Morrison Hill Technical Institute. He joined the Hong Kong Polytechnic in 1979 and his present post is Associate Professor of the Department of Mechanical Engineering. His research areas are: Fluid Mechanics, Flow visualization studies, Flows around cylinders-FIV, Numerical simulations.